Radiation Physics and Chemistry 166 (2020) 108490

Contents lists available at ScienceDirect

Radiation Physics and Chemistry

journal homepage: www.elsevier.com/locate/radphyschem

2D photon dosimetry with a scintillation fibre optic dosimeter

James Archer[a], Levi Madden[a], Enbang Li[a,*], Dean Wilkinson[b], Anatoly Rosenfeld[a,c]

[a] Centre for Medical Radiation Physics, University of Wollongong, Wollongong, NSW, 2522, Australia
[b] Illawarra Cancer Care Centre, Wollongong Hospital, Wollongong, NSW, 2500, Australia
[c] Illawarra Health and Medical Research Institute, University of Wollongong, Wollongong, NSW, 2522, Australia

ARTICLE INFO

Keywords:
Scintillator
2D dosimetry
CLINAC
Optical fibre

ABSTRACT

As part of clinical safety for radiation therapy, quality assurance is vital to ensure that the delivered dose matches the prescribed dose for any targeted volumes and surrounding healthy tissue. A challenge when measuring the beam quality, especially for smaller sized beams, is having a water equivalent dosimeter with a high spatial resolution and the ability to perform accurate 2D mapping. In this work we use a plastic scintillator fibre optic dosimeter to measure a 2D beam profile of a 6 MV CLINAC photon beam with field sizes $30 \times 30\,mm^2$ and $10 \times 10\,mm^2$. The results supplement commissioning dosimetry data measured with three commercial dosimeters – two ionisation chambers (Scanditronix/Wellhofer CC13 and CC01) and a diode detector (IBA PFD-3G diode). We find that the 2D scanning system can cover the entire larger field in 27 min using 2 mm steps, providing a quick and thorough mapping of the beam for quality assurance. This system allows the step size to be varied as desired, something arrayed detectors cannot do. We measure an average uncertainty of 1% inside the field and 5% outside the field, demonstrating this system as a viable method for thorough mapping of 2D fields and as a tool for complimenting ionisation chamber measurements in thorough clinical quality assurance.

1. Introduction

Scintillator fibre optic dosimetry was initially investigated for medical physics applications by Beddar et al. in 1992 (Beddar et al., 1992a, 1992b), where the authors optically coupled a cylindrical section of BC-400 plastic scintillator (Saint Gobain) onto a plastic optical fibre. The optical fibre was used to transport the optical photons generated by the scintillator to a photomultiplier tube (PMT). They found that the BC-400 scintillator was energy independent and water equivalent for photon and electron treatment beams, as well as being temperature independent (up to 60°C) and radiation resistant (<3% response decrease after 10 kGy). These properties make scintillator fibre optic dosimeters (FODs) very robust, and hence desirable dosimeters.

Since then a number of FODs have been investigated in photon (Kim et al., 2013; Archer et al., 2017a, 2017b; Masi et al., 2016) and electron (Beddar et al., 1992b; Lacroix et al., 2010) dosimetry, as well as brachytherapy (Rosenthal et al., 2003; Arnfield et al., 1996; Suchowerska et al., 2011) and eye plaque dosimetry (Bambynek et al., 1999). Two dimensional scintillator dosimetry has been explored using long lengths of scintillating fibre to assess clinical linear accelerator (CLINAC) leaf positioning errors (Goulet et al., 2011) by measuring the integral scintillation light along each fibre. Further, a system using an array of scintillating fibres rotated around the irradiating beam axis and analysed by tomodosimetry (conceptually similar to computed tomography) is able to reconstruct a two dimensional dose profile (Goulet et al., 2012).

The simplest method for 2D dosimetry is to use radiochromic film. This has a high spatial resolution but requires development, making real-time dosimetry impossible. Improvements in film techniques have been achieved with novel materials (such as Al_2O_3 (Ahmed et al., 2014) and optically stimulated luminescence (Wouter et al., 2017)) but still require development or processing to acquire dose information. These methods have resulted in sub-millimetre spatial resolutions. Liquid scintillator volumes measured with a CCD camera have been applied to 2D dosimetry, finding 2D profiles and PDDs (Pönisch et al., 2009). The authors achieved a gamma index (3%, 3 mm) in agreement of 96% within the field, but had issues with light scatter and total internal reflection from the liquid scintillator volume. Further, the measurements taken are not true 1D or 2D slices of the dose profiles, but are a net signal over the CCD camera axis.

Typically arrayed dosimeters are used for 2D mapping, which can provide a near-instant beam profile, but the detector pitch is limited by the volume of the detectors. A number of arrayed silicon diode detectors (Buonamici et al., 2007) and arrayed ionisation chambers (Stelljes et al., 2015) are available. A challenge when using arrayed detectors is

* Corresponding author.
E-mail address: enbang@uow.edu.au (E. Li).

https://doi.org/10.1016/j.radphyschem.2019.108490
Received 5 April 2019; Received in revised form 17 July 2019; Accepted 10 September 2019
Available online 12 September 2019
0969-806X/

ensuring that all the detectors are correctly calibrated to either each other, or to absolute dose. For example, arrayed diode detectors require correction factors to account for variations in sensitivity (Buonamici et al., 2007). The smallest detector pitch available is 2.47 mm with the Sun Nuclear SRS Mapcheck (Sun Nuclearatient, 1119).

Due to their large volumes, ionisation chambers are not appropriate for small-field applications, where volume-averaging effects will cause a blurring of measured dose. Their large volumes also make tightly packed arrays challenging and limits the minimum pitch. Silicon diodes are able to be manufactured to have a small sensitive volume, but lack direction and temperature independence (Colussi et al., 2001), and require extensive calibration for different beam setups and energies (Meiler and Podgorsak, 1997). The beam perturbations of arrays must also be considered.

FODs can be fabricated to have a sensitive volume of any size, limited only by light detection sensitivity, and so are an ideal tool for high spatial resolution dosimetry. FOD arrays have been used for 2D dosimetry. Notably, an array of 781 FODs over a 26 cm × 26 cm grid, measured simultaneously with a CCD camera, achieving a 1% precision of dose measurement (Guillot et al., 2011).

In this work we present two-dimensional dose profiles that are measured using a single scintillator probe translated through the beam. By sacrificing a larger number of scintillator fibres, we achieve a simpler setup and minimise the volume of material to be moved throughout the field. With the goal of high accuracy, a scintillator volume is used to minimise both the dose blurring in the edge of the field and the dose perturbation by having a large number of fibres in the field (Goulet et al., 2011).

The primary source of unwanted signal in scintillator dosimetry is Cherenkov radiation. This is an optical effect caused by charged particles travelling faster than the local speed of light. In a plastic (such as the fibre optic core) this corresponds to an electron energy of 175 keV. Hence in high-energy photon or electron dosimetry Cherenkov radiation will be generated in both the plastic scintillator as well as the optical fibre. The Cherenkov radiation generated inside the optical fibre and scintillator itself will compromise the spatial resolution of the detector and so must be removed. Beddar et al. described a method to measure and remove the Cherenkov radiation, which uses a second fibre optic with no scintillator to measure only the Cherenkov radiation produced in the optical fibre, which is measured with a second PMT. This signal can be subtracted from the PMT response of the scintillator probe yielding the signal of interest (Beddar et al., 1992a). This background subtraction method is considered the “gold standard” in the field of scintillator dosimetry.

2. Methods

The sensitive volume of our dosimeter probe was made with BC-444 plastic scintillator (Saint-Gobain Crystals). The scintillator sensitive volume is a cylinder 0.5 mm long and 2.2 mm in diameter. The scintillator was cut to the approximate volume, and then polished with optical grade polish paper to the required dimensions, which also ensures optimal coupling and internal reflection. When coupled to an Eska CK-40 plastic optical fibre with silicone optical grease, which has a core diameter of 1 mm and shielding diameter of 2 mm, a total sensitive volume of 0.39 mm^2 can have light captured into the optical fibre. A second probe was made without scintillator on the end to measure the Cherenkov only signal. This probe was located below the scintillator probe (with respect to the incoming beam) so that they were laterally in the same position. This gave the probes a centre-to-centre distance of 2.2 mm. As measurements were performed at 15 mm depth (d_{max}), the dose gradient over this 2.2 mm is minimal. Both probes were coated in a TiO_2 reflective paint to improve light capture and prevent external light leaking into the optical fibre. A diagram of the scintillator probe is shown in Fig. 1.

Two RCA-4526 PMTs were used as photodetectors. The PMT voltage

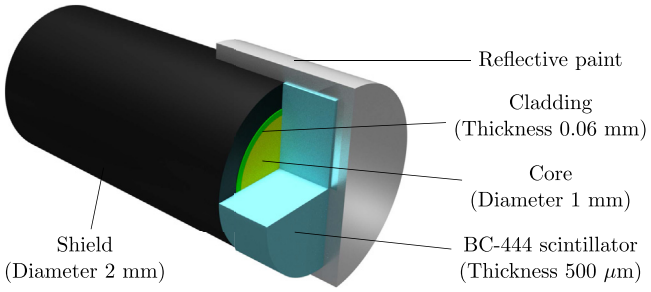

Fig. 1. Diagram of the scintillator fibre-optic dosimeter, showing the optical fibre, scintillator and reflective paint. Not to scale.

signal was digitised with a PS-6404D oscilloscope. Two channels were measured: the PMT response from the scintillator probe, and the PMT response from the Cherenkov probe. A third channel acted as the trigger, which was linked to the CLINAC transistor-transistor logic (TTL) pulse. The data were sampled with a 1.6 ns sample period (625 MHz sample frequency). 100 integral measurements of individual 17.6 μs CLINAC pulses were acquired at each position and averaged to reduce noise. The oscilloscope channels were AC coupled so that any DC offset or potential constant light leakage is removed from the results.

To acquire the total relative dose at a position, the PMT response waveform was zeroed (by subtracting the average of the first 1000 samples (1.6 μs) from the entire waveform) then the sum was taken to get the total PMT response (in units of volts) for the pulses. The same is done for the Cherenkov probe response, and the difference is the net scintillator response in the field. The primary difficulty with this method is calibration between the two PMTs: different PMT gains give a different voltage response for the same signal. To correct for this the response of both channels subjected to the same light signal is measured. The signal from both the fibres (one with the scintillator and one without) can be used for this. The scintillator probe was attached to PMT 1 and the Cherenkov probe to PMT 2 and the signal recorded (S_1 and C_2 respectively). These were then swapped to the scintillator probe was attached to PMT 2 and the Cherenkov probe to PMT 1 (S_2 and C_1 respectively). This allows the ratio of the gains to be calculated as follows using the two signals:

$$\text{Calibration factor} = \frac{S_1}{S_2} = \frac{C_1}{C_2} \tag{1}$$

This gives two values for the ratio of signals from PMT 1 and PMT 2. To combine these, the two values are combined geometrically:

$$\text{Calibration factor} = \sqrt{\frac{S_1}{S_2} \times \frac{C_1}{C_2}} \tag{2}$$

The uncertainty in this value was found using the standard deviation of the individual calibration factor. The resulting calibration factor can simply be multiplied by the Cherenkov response (the channel 2 data) to properly calculate the net scintillator output. A Varian 21iX CLINAC (located at the Illawarra Cancer Care Centre, Wollongong Hospital) was used to generate the photon beam. The CLINAC accelerating potential was 6 MV, corresponding to photons with maximum energy of 6 MeV. The probes were scanned through the beam using two Thorlabs LTS-150 translation stages, mounted perpendicular to each other. The stages were synchronised with the PS-6404D and controlled with a LabView 2015 program to automate the scanning and data acquisition process. The scan step size and number of averages at each point (set to 100 for the 2D scans) are able to be varied in the program. The measurements were done using a 30 cm × 30 cm × 15 cm Gammex RMI Solid Water phantom, with source-to-surface distance 100 cm with the probe depth at 15 mm (d_{max} at 6 MV). Two field sizes were measured: 30 × 30 mm^2 and 10 × 10 mm^2 (square fields with areas 900 mm^2 and 100 mm^2 respectively).

Table 1
Dosimeter resolution information. Note that the FOD and IC are cylinders that present a rectangular cross-section to the field, while the diode is a cylinder that presents a circular cross-section to the field.

Detector	FOD	CC13	CC01	Diode
Diameter (XP) (mm)	1.0	6.0	2.0	2.0
Length (IP) (mm)	0.5	5.8	3.6	2.0
Sensitive volume (mm^3)	0.39	130	10	0.19

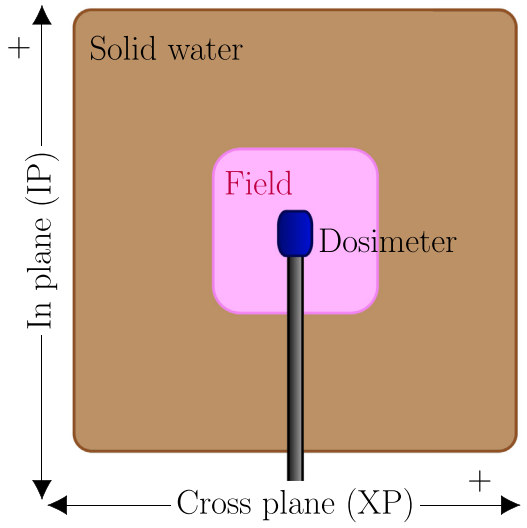

Fig. 2. Diagram of the dosimeter setup from above. The reference probe is located beneath the FOD. Cross plane (XP) is defined as left to right, In plane (IP) is defined as down to up.

Table 2
Interpolated penumbra width measured with the dosimeters in the two fields. The uncertainties are ± 0.1 mm.

	Penumbra (mm)						
	$30 \times 30\ mm^2$			$10 \times 10\ mm^2$			
	FOD	CC13	Diode	FOD	CC13	CC01	Diode
Left (-XP)	4.3	4.8	2.6	3.6	5.2	3.3	3.2
Right (+XP)	4.4	4.8	2.6	3.8	5.1	3.4	3.2
Bottom (-IP)	2.7	–	–	2.9	–	–	2.5
Top (+IP)	2.9	–	–	2.9	–	–	2.5

Two dimensional scanning through the fields were done in steps of 2 mm steps for the $30 \times 30\ mm^2$ field over a distance of 50 mm (in both directions). For the $10 \times 10\ mm^2$ field the step size was 1 mm, over a 20 mm range. This allowed the field to be well sampled while also measuring the out-of-field response. To assess the repeatability, the probe was scanned in one dimension across the $10 \times 10\ mm^2$ field four times.

We compared to commissioning dosimetry from three standards used for quality assurance of this CLINAC. Two Scanditronix/Wellhofer ionisation chambers (IC): CC13 and CC01, and a IBA PFD-3G diode. The sensitive volume properties of these detectors, as well as the scintillator FOD, are presented in Table 1. The differences in sensitive volumes will be most apparent in the smaller sized fields explored in this work.

The arrangement of the dosimeters relative to the field, and definitions of the coordinates, is shown in Fig. 2. One dimensional beam profiles had been measured with these dosimeters. Reference dosimetry from the CLINAC commissioning was not measured at the time for each dosimeter in each field. CC01 data was acquired in the $10 \times 10\ mm^2$ field due to its smaller sensitive volume than the CC13, and In plane data was measured here with the Diode to assess field symmetry. A summary of which data was available can be found in Table 2.

3. Results

The calibration of the two PMTs resulted in two values of 1.358 and 1.386, giving a (geometrically) averaged value of 1.372 ± 0.014. These values were calculated from the values $S_1 = 10.05$, $S_2 = 7.40$, $C_1 = 0.896$, $C_2 = 0.646$.

A plot of the 2D scans measured with the FOD are shown in Fig. 3, with cross sections of the XP and IP profiles presented in Fig. 4. Table 2 shows the field penumbra with the different detectors in the two field sizes, calculated from the data in Fig. 4. The penumbra were calculated by finding the distance for the dose to rise from 20% maximum to 80%. The response was cubically interpolated between measurement points with 0.1 mm samples to find the 20%–80% positions.

There are two sources of uncertainty in the FOD results: calibration uncertainty and repeatability of the FOD measurements. The calibration error is 1%. The repeatability of the FOD was investigated with the four repeated scans. The results match very closely with each other, with the relative differences to the mean response presented in Fig. 5 (a). These responses have not been normalised so these are a direct comparison of the absolute responses. This demonstrates the short-term stability of the PMT gains. The average relative difference from the mean is 1.4%. It is smaller inside the field (−5 mm–5 mm) with only 0.27% difference. Outside the field, the average is 1.9%. The most extreme difference is 12.5% below the mean, on the edge of the field, but the vast majority of the values are within ±5%. The 95% confidence interval for the repeatability is 4.65%, however this will overestimate

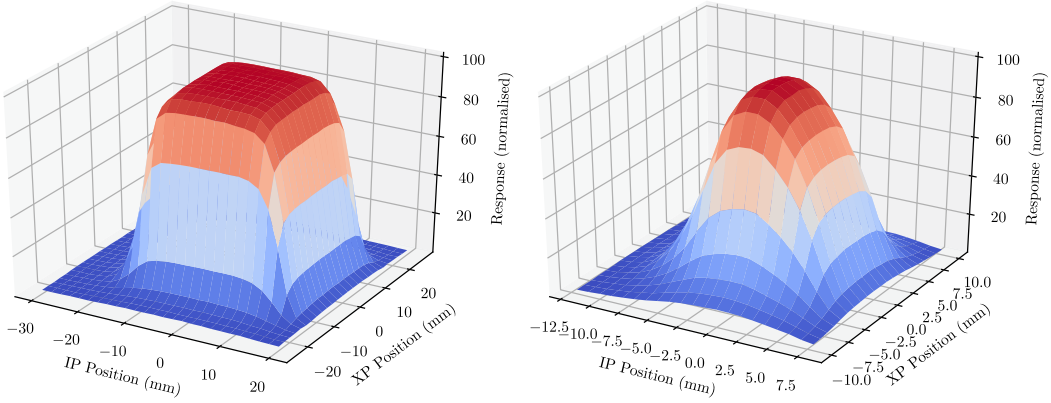

Fig. 3. Experimental 2D scans of the two field sizes measured with the FOD. Left: $30 \times 30\ mm^2$. Right: $10 \times 10\ mm^2$.

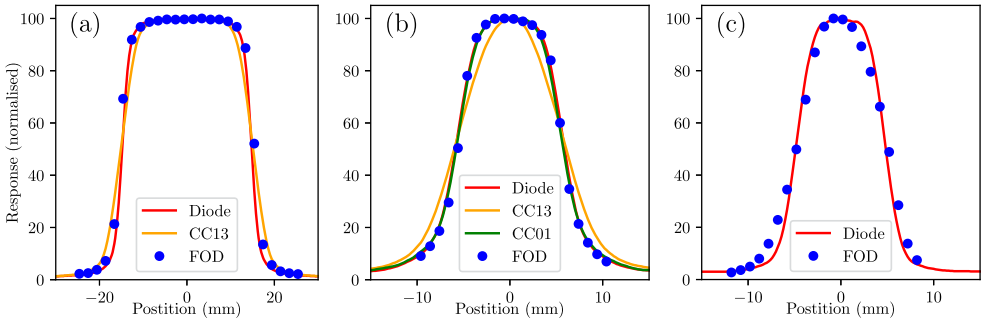

Fig. 4. Beam profiles compared to the ion chambers and diode results. (a) 30 × 30 mm^2 XP. (b) 10 × 10 mm^2 XP. (c) 10 × 10 mm^2 IP.

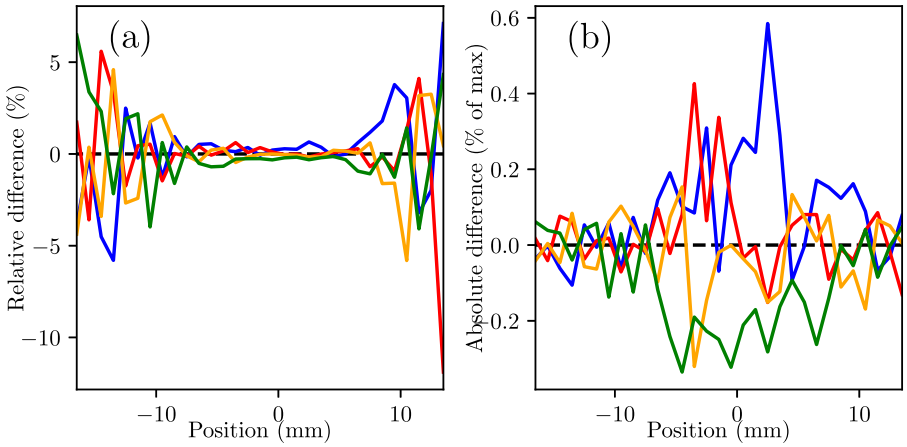

Fig. 5. Four IP scans using the FOD in the 10 × 10 mm^2 field. The differences to the mean response are shown here, as (a) as a percent of the relative mean response and (b) a percent of the maximum mean response.

the uncertainty of the values inside the field, which are much more accurate than this. Using the difference to the maximum of the mean, Fig. 5(b), (rather than relative to the response at the point) we get an average difference to the mean of 0.1%, relative to the centre of the field. This has a 95% confidence interval of 0.28%. Combining this with the calibration uncertainty, the overall uncertainty is $\sqrt{1\%^2 + 0.28\%^2} = 1.04\%$. This is too small to show effectively on Fig. 4.

4. Discussion

It can be seen in Fig. 4 that the FOD results match very closely to the diode results, with some slight discrepancies in the penumbra due to volume averaging. The volume averaging effect of the larger sensitive volumes is most apparent in Fig. 4(b), where the CC13 does not match the response of the other devices. Fig. 4(b) indicates that, as all dosimeters agree except the CC13, that the roll-off in the 10 × 10 mm^2 is large enough for the CC01 to be valid, despite the size of the chamber. There is a discrepancy between the FOD and diode results in the 10 × 10 mm^2 field when scanned IP (Fig. 4(c)). Despite the FOD having a higher resolution in this direction (0.5 mm versus 1 mm) there is an asymmetry in the probe: one side is the reflective paint, and the other side is the optical fibre. We hypothesise that this is the cause of the slight over-response on the negative position: the higher-Z titanium scatters more secondary electrons in the field into the scintillator volume, causing a higher dose to be deposited than would be expected. As there is less paint on the other side we do not see this at positive positions. This discrepancy seen in the IP profile (but not in the XP profile in the same field) points to the limit in field size appropriate for this detector. In a clinical setting, scanning through a field 10 × 10 mm^2 or smaller should be performed with the FOD aligned edge-on to the direction of scanning.

The different approaches for quantifying the uncertainty leads to two different values: 1.04% and 4.76% (calculated the same way by combining 1% and 4.65% in quadrature). The first value is more appropriate for inside the field, and the second for in the regions of lower dose. Hence we can summarise the accuracy of the FOD as within 1% inside the field, and within 5% outside. This choice of uncertainty quantification uses the largest uncertainty in each region, showing the worst-case of the system. This uncertainty is approximately twice the IC measurements, which are repeatable within 0.5% within the field and 2% outside. Ideally the out of field data should be within 3%, so the FOD 1D cross-section results must be validated against IC beam profiles. This will in turn validate the 2D data across the field.

The total time to perform the scans were 27 min for large field (676 positions), and 17 min for small field (441 positions) at an average of 2.35 s per position. The primary use of time during the data collection is sending the data from the PS6404 to the laptop. The CLINAC pulse frequency is 370 Hz so over 100 averages this will take (at a minimum) 0.27 s. Field size and desired resolution are the key factors in the scan times. The programmable resolution and number of measurements makes this system robust to the specific measurement being taken, unlike fixed array detectors. While their results can be acquired nearly instantaneously, the variable pitch (in both directions) of the FOD scanning system provides more freedom at the expense of scan time. 1 mm steps were used here, but there is no intrinsic minimal step size with this setup. While the scan time is not optimal for daily or weekly clinical QA, it is appropriate for less frequent but more thorough dosimetry. By optimising the scanning route, unnecessary transit times can be minimised, but appropriate parameters for a given measurement will provide the best timing to resolution optimisation.

5. Conclusions

In this work we have demonstrated the ability for a fibre-optic

dosimeter to perform accurate 2D measurements CLINAC photon fields. By comparing it to two ionisation chambers and a diode detector, we assess that the detector has a comparable ability to perform dosimetry to the CC01 and diode detectors. We show that it has a higher spatial resolution to a CC13 ionisation chamber, with significant improvements to the measured beam penumbra. The data acquisition system used allows the 2D beam profiles to be measured with a robust effective detector pitch in a reasonable time, providing a system that can compliment ionisation chamber measurements as part of a comprehensive clinical QA.

Declarations of interest

None.

Acknowledgements

This research has been conducted with the support of the Australian Government Research Training Program Scholarship.

References

Ahmed, M., Eller, S., Schnell, E., Ahmad, S., Akselrod, M., Hanson, O., Yukihara, E., 2014. Development of a 2D dosimetry system based on the optically stimulated luminescence of Al^2O^3. Radiat. Meas. 71, 187–192.

Archer, J., Li, E., Petasecca, M., Lerch, M., Rosenfeld, A., Carolan, M., 2017a. High-resolution fiber-optic dosimeters for microbeam radiation therapy. Med. Phys. 44 (5), 1965–1968.

Archer, J., Madden, L., Li, E., Carolan, M., Petesecca, M., Metcalfe, P., Rosenfeld, A., 2017b. Temporally separating cherenkov radiation in a scintillator probe exposed to a pulsed x-ray beam. Phys. Med. 42, 185–188.

Arnfield, M.R., Gaballa, H.E., Zwicker, R.D., Islam, Q., Schmidt-Ullrich, R., 1996. Radiation-induced light in optical fibers and plastic scintillators: application to brachytherapy dosimetry. IEEE Trans. Nucl. Sci. 43 (3), 2077–2084.

Bambynek, M., Flühs, D., Heintz, M., Kolanoski, H., Wegener, D., Quast, U., 1999. Fluorescence ^{125}I eye applicator. Med. Phys. 26 (11), 2476–2481.

Beddar, A.S., Mackie, T.R., Attix, F.H., 1992a. Water-equivalent plastic scintillation detectors for high-energy beam dosimetry: 1. Physical characteristics and theoretical considerations. Phys. Med. Biol. 37 (10), 1883–1900.

Beddar, A.S., Mackie, T.R., Attix, F.H., 1992b. Water-equivalent plastic scintillation detectors for high-energy beam dosimetry: 2. Properties and measurements. Phys. Med. Biol. 37 (10), 1901–1913.

Buonamici, F.B., Compagnucci, A., Marrazzo, L., Russo, S., Bucciolini, M., 2007. An intercomparison between film dosimetry and diode matrix for IMRT quality assurance. Med. Phys. 34 (4), 1372–1379.

Colussi, V.C., Beddar, A.S., Kinsella, T.J., Sibata, C.H., 2001. In vivo dosimetry using a single diode for megavoltage photon beam radiotherapy: implementation and response characterization. J. Appl. Clin. Med. Phys. 2 (4), 210–218.

Goulet, M., Gingras, L., Beaulieu, L., 2011. Real-time verification of multileaf collimator-driven radiotherapy using a novel optical attenuation-based fluence monitor. Med. Phys. 38 (3), 1459–1467.

Goulet, M., Archambault, L., Beaulieu, L., Gingras, L., 2012. High resolution 2D dose measurement device based on a few long scintillating fibers and tomographic reconstruction a. Med. Phys. 39 (8), 4840–4849.

Guillot, M., Beaulieu, L., Archambault, L., Beddar, S., Gingras, L., 2011. A new water-equivalent 2D plastic scintillation detectors array for the dosimetry of megavoltage energy photon beams in radiation therapy. Med. Phys. 38 (12), 6763–6774.

Kim, K.A., Yoo, W.J., Jang, K.W., Moon, J., Han, K.T., Jeon, D., Park, J.Y., Cha, E.J., Lee, B., 2013. Development of a fibre-optic dosemeter to measure the skin dose and percentage depth dose in the build-up region of therapeutic photon beams. Radiat. Prot. Dosim. 153 (3), 294–299.

Lacroix, F., Guillot, M., McEwen, M., Cojocaru, C., Gingras, L., Beddar, A.S., Beaulieu, L., 2010. Extraction of depth-dependent perturbation factors for parallel-plate chambers in electron beams using a plastic scintillation detector. Med. Phys. 37 (8), 4331–4342.

Masi, L., Russo, S., Francescon, P., Doro, R., Frassanito, M.C., Fumagalli, M.L., Reggiori, G., Marinelli, M., Redaelli, I., Pimpinella, M., Verona Rinati, G., Siragusa, C., Vigorito, S., Mancosu, P., 2016. Cyberknife beam output factor measurements: a multi-site and multi-detector study. Phys. Med.: Eur. J. Med. Plants 32 (12), 1637–1643.

Meiler, R.J., Podgorsak, M.B., 1997. Characterization of the response of commercial diode detectors used for in vivo dosimetry. Med. Dosim. 22 (1), 31–37.

Pönisch, F., Archambault, L., Briere, T.M., Sahoo, N., Mohan, R., Beddar, S., Gillin, M.T., 2009. Liquid scintillator for 2D dosimetry for high-energy photon beams. Med. Phys. 36 (5), 1478–1485.

Rosenthal, P., Weber, W., Forster, A., Orth, O., Kohler, B., Seiler, F., 2003. Calibration and validation of a quality assurance system for 90sr/90y radiation source trains. Phys. Med. Biol. 48 (5), 573–585.

Stelljes, T.S., Harmeyer, A., Reuter, J., Looe, H.K., Chofor, N., Harder, D., Poppe, B., 2015. Dosimetric characteristics of the novel 2D ionization chamber array OCTAVIUS Detector 1500. Med. Phys. 42 (4), 1528–1537.

Suchowerska, N., Jackson, M., Lambert, J., Yin, Y.B., Hruby, G., McKenzie, D.R., 2011. Clinical trials of a urethral dose measurement system in brachytherapy using scintillation detectors. Int. J. Radiat. Oncol. Biol. Phys. 79 (2), 609–615.

Sun nuclear, SRS patient QA, No film. https://www.sunnuclear.com/documents/datasheets/SRSMapCHECK061119.pdf, Accessed date: 15 June 2019.

Wouter, C., Dirk, V., Paul, L., Tom, D., 2017. A reusable OSL-film for 2D radiotherapy dosimetry. Phys. Med. Biol. 62 (21), 8441.